J|A|C|S ARTICLES

Published on Web 10/18/2010

Hydrophobic Self-Assembly of a Perylenediimide-Linked DNA Dumbbell into Supramolecular Polymers

Prakash P. Neelakandan,[†] Zhengzheng Pan,[†] Mahesh Hariharan,[†,‡] Yan Zheng,[†] Haim Weissman,[§] Boris Rybtchinski,*[,§] and Frederick D. Lewis*[,†]

Department of Chemistry, Northwestern University, Evanston, Illinois 60208, United States, School of Chemistry, Indian Institute of Science Education and Research Thiruvananthapuram, Kerala, India 695016, and Department of Organic Chemistry, Weizmann Institute of Science, Rehovot 76100, Israel

Received August 24, 2010; E-mail: fdl@northwestern.edu; boris.rybtchinski@weizmann.ac.il

Abstract: The self-assembly of DNA dumbbell conjugates possessing hydrophobic perylenediimide (PDI) linkers separated by an eight-base pair A-tract has been investigated. Cryo-TEM images obtained from dilute solutions of the dumbbell in aqueous buffer containing 100 mM NaCl show the presence of structures corresponding to linear end-to-end assemblies of 10−30 dumbbell monomers. The formation of assemblies of this size is consistent with analysis of the UV−vis and fluorescence spectra of these solutions for the content of PDI monomer and dimer chromophores. Assembly size is dependent upon the concentration of dumbbell and salt as well as the temperature. Kinetic analysis of the assembly process by means of salt-jump stopped-flow measurements shows that it occurs by a salt-triggered isodesmic mechanism in which the rate constants for association and dissociation in 100 mM NaCl are 3.2×10^7 $M^{-1}s^{-1}$ and 1.0 s^{-1}, respectively, faster than the typical rate constants for DNA hybridization. TEM and AFM images of samples deposited from solutions having higher concentrations of dumbbell and NaCl display branched assemblies with linear regions >1 μm in length and diameters indicative of the formation of small bundles of dumbbell end-to-end assemblies. These observations provide the first example of the use of hydrophobic association for the assembly of small DNA duplex conjugates into supramolecular polymers and larger branched aggregates.

Introduction

Traditional strategies for the linear assembly of DNA-based materials are dependent upon Watson−Crick base pairing.[1] Assembly of oligomers having repeating units can be accomplished using either thermodynamic base pairing of single strand regions ("sticky ends")[2,3] or by kinetically controlled self-assembly.[4] Base pairing can also be used to assemble linear oligomers containing repeating organic molecules.[5] Further assembly of duplex DNA into larger linear fibers generally requires high concentrations of duplex and the use of organic or inorganic di- or polycations.[6] DNA nanofibers can also be prepared by self-assembly of DNA block copolymers.[7] End-to-end duplex assembly based on hydrophobic association of terminal base pairs is observed at high concentrations in single crystals[8] and in liquid crystals but not in dilute solution.[9,10] Hydrophobic self-assembly of guanine tetrads has been employed for the preparation of well-defined G-quadruplex assemblies.[11] However, hydrophobic association has not been employed for the assembly of linear DNA supramolecular polymers.

[†] Northwestern University.
[‡] Indian Institute of Science Education and Research Thiruvananthapuram.
[§] Weizmann Institute of Science.

(1) (a) Storhoff, J. J.; Mirkin, C. A. *Chem. Rev.* **1999**, *99*, 1849–1862. (b) Gothelf, K. V.; LaBean, T. H. *Org. Biomol. Chem* **2005**, *3*, 4023–4037. (c) Pitchiaya, S.; Krishnan, Y. *Chem. Soc. Rev.* **2006**, *35*, 1111–1121. (d) Kwon, Y. W.; Lee, C. H.; Choi, D. H.; Jin, J. I. *J. Mater. Chem.* **2009**, *19*, 1353–1380. (e) Modi, S.; Bhatia, D.; Simmel, F. C.; Krishnan, Y. *J. Phys. Chem. Lett.* **2010**, *1*, 1994–2005.
(2) (a) Aldaye, F. A.; Palmer, A. L.; Sleiman, H. F. *Science* **2008**, *321*, 1795–1799. (b) Seeman, N. C. *Annu. Rev. Biophys. Biomol. Struct.* **1998**, *27*, 225–248. (c) Seeman, N. C. *Nature* **2003**, *421*, 427–431.
(3) Jing, T. W.; Jeffrey, A. M.; Derose, J. A.; Lyubchenko, Y. L.; Shlyakhtenko, L. S.; Harrington, R. E.; Appella, E.; Larsen, J.; Vaught, A.; Rekesh, D.; Lu, F. X.; Lindsay, S. M. *Proc. Natl. Acad. Sci. U.S.A.* **1993**, *90*, 8934–8938.
(4) Lubrich, D.; Green, S. J.; Turberfield, A. J. *J. Am. Chem. Soc.* **2009**, *131*, 2422–2423.
(5) (a) Waybright, S. M.; Singleton, C. P.; Wachter, K.; Murphy, C. J.; Bunz, U. H. F. *J. Am. Chem. Soc.* **2001**, *123*, 1828–1833. (b) Abdalla, M. A.; Bayer, J.; Radler, J. O.; Müllen, K. *Angew. Chem., Int. Ed.* **2004**, *43*, 3967–3970.
(6) (a) Bloomfield, V. A. *Curr. Opin. Struct. Biol.* **1996**, *6*, 334–341. (b) Li, Y.; Yildiz, U. H.; Mullen, K.; Grohn, F. *Biomacromolecules* **2009**, *10*, 530–540.
(7) Carneiro, K. M. M.; Aldaye, F. A.; Sleiman, H. F. *J. Am. Chem. Soc.* **2010**, *132*, 679–685.
(8) Lewis, F. D.; Liu, X.; Wu, Y.; Miller, S. E.; Wasielewski, M. R.; Letsinger, R. L.; Sanishvili, R.; Joachimiak, A.; Tereshko, V.; Egli, M. *J. Am. Chem. Soc.* **1999**, *121*, 9905–9906.
(9) Livolant, F.; Levelut, A. M.; Doucet, J.; Benoit, J. P. *Nature* **1989**, *339*, 724–726.
(10) Nakata, M.; Zanchetta, G.; Chapman, B. D.; Jones, C. D.; Cross, J. O.; Pindak, R.; Bellini, T.; Clark, N. A. *Science* **2007**, *318*, 1276–1279.
(11) (a) Davis, J. T.; Spada, G. P. *Chem. Soc. Rev.* **2007**, *36*, 296–313. (b) Gonzalez-Rodriguez, D.; Janssen, P. G. A.; Martin-Rapun, R.; De Cat, I.; De Feyter, S.; Schenning, A. P. H. J.; Meijer, E. W. *J. Am. Chem. Soc.* **2010**, *132*, 4710–4719. (c) Gonzalez-Rodriguez, D.; van Dongen, J. L. J.; Lutz, M.; Spek, A. L.; Schenning, A. P. H. J.; Meijer, E. W. *Nature Chem.* **2009**, *1*, 151–155.

 10.1021/ja1076525

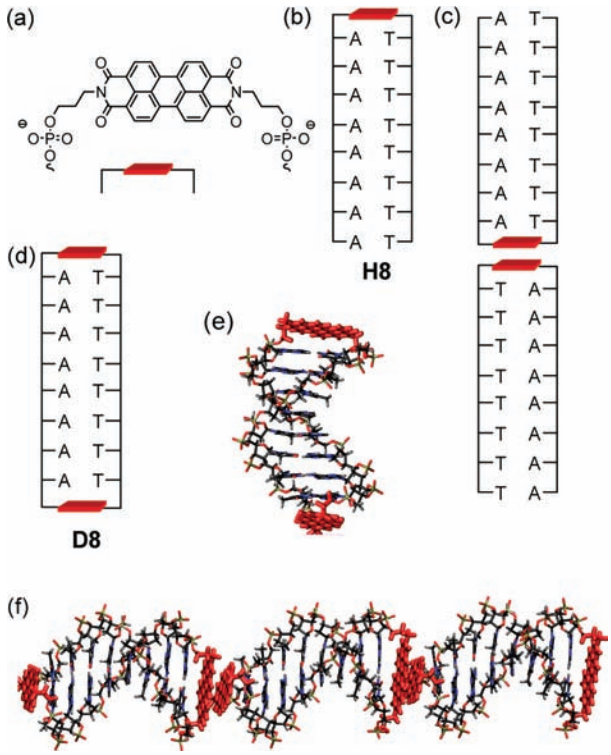

Figure 1. Structures of (a) the PDI linker, (b) hairpin **H8**, (c) hairpin dimer, (d) dumbbell **D8**, (e) energy minimized structure of **D8**, and (f) schematic representation of a **D8** trimer depicting end-to-end association.

Aggregation of the planar hydrophobic aromatic molecule perylenediimide (PDI) has been extensively employed in studies of molecular self-assembly.[12−15] Incorporation of PDI into oligonucleotide conjugates is reported to result in intra- and intermolecular hydrophobic association of the chromophores in single strand,[16] duplex,[17,18] hairpin,[19] and hairpin dimer structures.[17,20,21] We recently reported that the conjugate **H8** which possesses a PDI hairpin linker (Figure 1a) exists as a monomer in water (Figure 1b), but forms a dimer in the presence

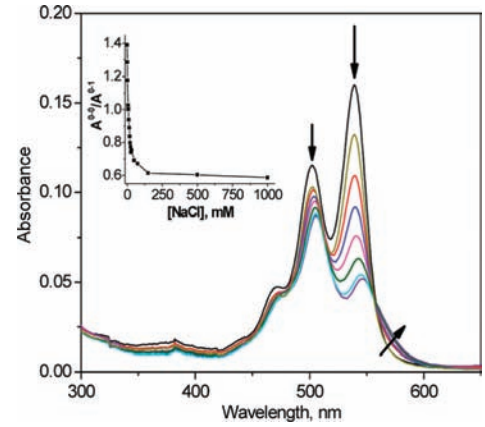

Figure 2. NaCl concentration dependent changes in the UV−vis spectra of 1.0 μM **D8** in 10 mM phosphate buffer (pH 7.2). Arrows show effect of increasing NaCl concentration. Inset shows the ratio of vibronic bands A^{0-0}/A^{0-1} vs NaCl concentration.

of NaCl (Figure 1c).[22] Thus, dumbbell structures possessing a PDI-linker at both ends might undergo end-to-end assembly. We report here the results of our collaborative investigation of the assembly of the PDI-linked dumbbell conjugate **D8** (Figure 1d,e), which possesses an 8-mer A-tract duplex base pair domain. A-tracts have been employed in our previous studies of **H8** dimerization and hole transport in PDI−DNA conjugates;[21,22] however, self-assembly of dumbbells is not dependent upon the use of an A-tract base pair domain. The conjugate **D8** forms linear end-to-end assemblies (Figure 1f) as long as 100 nm (30 monomers) in dilute solution, as characterized by cryo-TEM. The assembly process occurs by a salt-triggered isodesmic supramolecular polymerization mechanism.[15,23] When cast from dilute solution **D8** assembles into branched fibers with linear segments longer than 1 μm.

Results

Dumbbell Structure and Electronic Spectra. The synthesis and characterization of monomeric **D8** has been reported.[24] Molecular modeling of the monomeric dumbbell is consistent with a B-DNA A-tract with π-stacking between the terminal base pairs and the adjacent PDI linker (Figure 1e).[24] The long-wavelength regions of the UV−visible absorption spectra of 1 μM **D8** in 10 mM sodium phosphate buffer (pH 7.2, Na^+ concentration 17 mM) in the absence and presence of added 0−1.0 M NaCl are shown in Figure 2 and the entire UV−vis spectra are shown in Figure S1 (Supporting Information). The long-wavelength absorption band in buffer has a vibronic band structure similar to that for isolated PDI chromophores and has an A^{0-0}/A^{0-1} band intensity ratio of 1.4:1.[22,24,25] Absorption bands at shorter wavelength are assigned to nucleobase absorption overlapping with weaker PDI absorption (Figure S1). Addition of NaCl to **D8** in buffer results in a decrease in the A^{0-0}/A^{0-1} band intensity ratio and broadening of the UV spectrum (Figure 2). At high salt concentrations the spectrum

(12) Würthner, F.; Thalacker, C.; Diele, S.; Tschierske, C. *Chem.—Eur. J.* **2001**, *7*, 2245–2253.
(13) (a) Li, A. D. Q.; Wang, W.; Wang, L. *Chem.—Eur. J.* **2003**, *9*, 4594–4601. (b) Tang, T. J.; Qu, J.; Mullen, K.; Webber, S. E. *Langmuir* **2006**, *22*, 7610–7616. (c) Zang, L.; Che, Y.; Moore, J. S. *Acc. Chem. Res.* **2008**, *41*, 1596–1608.
(14) (a) Würthner, F. *Chem. Commun.* **2004**, 1564–1579. (b) Baram, J.; Shirman, E.; Ben-Shitrit, N.; Ustinov, A.; Weissman, H.; Pinkas, I.; Wolf, S. G.; Rybtchinski, B. *J. Am. Chem. Soc.* **2008**, *130*, 14966–14967. (c) Zhang, X.; Rehm, S.; Safont-Sempere, M. M.; Wurthner, F. *Nature Chem.* **2009**, *1*, 623–629.
(15) De Greef, T. F. A.; Smulders, M. M. J.; Wolffs, M.; Schenning, A. P. H. J.; Sijbesma, R. P.; Meijer, E. W. *Chem. Rev.* **2009**, *109*, 5687–5754.
(16) Wang, W.; Wan, W.; Zhou, H. H.; Niu, S. Q.; Li, A. D. Q. *J. Am. Chem. Soc.* **2003**, *125*, 5248–5249.
(17) Zheng, Y.; Long, H.; Schatz, G. C.; Lewis, F. D. *Chem. Commun.* **2005**, 4795–4797.
(18) (a) Ustinov, A. V.; Dubnyakova, V. V.; Korshun, V. A. *Tetrahedron* **2008**, *64*, 1467–1473. (b) Baumstark, D.; Wagenknecht, H. A. *Chem.—Eur. J.* **2008**, *14*, 6640–6645. (c) Baumstark, D.; Wagenknecht, H. A. *Angew. Chem., Int. Ed.* **2008**, *47*, 2612–2614.
(19) Zeidan, T. A.; Hariharan, M.; Siegmund, K.; Lewis, F. D. *Photochem. Photobiol. Sci.* **2010**, *9*, 916–922.
(20) Zheng, Y.; Long, H.; Schatz, G. C.; Lewis, F. D. *Chem. Commun.* **2006**, 3830–3832.
(21) Carmieli, R.; Zeidan, T. A.; Kelley, R. F.; Mi, Q.; Lewis, F. D.; Wasielewski, M. R. *J. Phys. Chem. A* **2009**, *113*, 4691–4700.
(22) Hariharan, M.; Zheng, Y.; Long, H.; Zeidan, T. A.; Schatz, G. C.; Vura-Weis, J.; Wasielewski, M. R.; Zuo, X. B.; Tiede, D. M.; Lewis, F. D. *J. Am. Chem. Soc.* **2009**, *131*, 5920–5929.
(23) Zhao, D. H.; Moore, J. S. *Org. Biomol. Chem.* **2003**, *1*, 3471–3491.
(24) Hariharan, M.; Siegmund, K.; Zheng, Y.; Long, H.; Schatz, G. C.; Lewis, F. D. *J. Phys. Chem. C* **2010**, DOI: 10.1021/jp1048309.
(25) Giaimo, J. A.; Lockard, J. V.; Sinks, L. E.; Scott, A. M.; Wilson, T. M.; Wasielewski, M. R. *J. Phys. Chem. A* **2008**, *112*, 2322–2330.

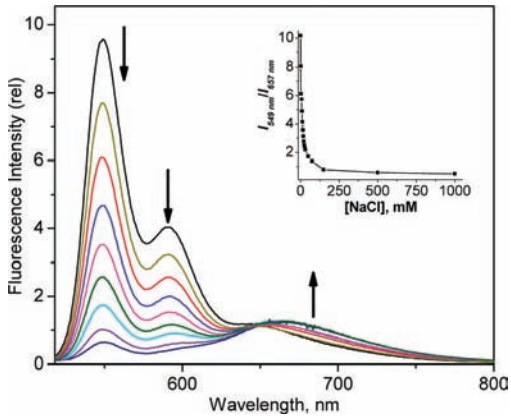

Figure 3. NaCl concentration dependent changes in the fluorescence spectra of 1.0 μM **D8** in 10 mM phosphate buffer (pH 7.2). Arrows show effect of increasing NaCl concentration. Inset shows the relative ratio of $I_{549\ nm}$ and $I_{657\ nm}$ band intensity vs NaCl concentration.

is characteristic of face-to-face PDI stacking.[22,25,26] A plot of the A^{0-0}/A^{0-1} band intensity ratio vs the concentration of added NaCl is shown in the inset of Figure 2. The UV spectrum of **D8** is dependent upon its concentration and the temperature. The spectra of 0.6−2.6 μM **D8** in buffer with 12 mM added NaCl are shown in Figure S2 (Supporting Information). Increasing **D8** concentration results in a decrease in the A^{0-0}/A^{0-1} ratio from 1.1 to 0.86, indicative of an increase in the PDI dimer/monomer ratio. Increasing the temperature from 0 to 50 °C results in an increase in the A^{0-0}/A^{0-1} ratio (indicating disaggregation), as shown in Figure S3 (Supporting Information) for solutions of **D8** in buffer with 12 and 100 mM added NaCl.

The fluorescence spectrum in buffer (Figure 3) displays a vibronic progression similar to that reported for monomeric PDI derivatives with a 0,0 band at 549 nm.[24] Addition of NaCl results in reduced intensity of the structured monomer fluorescence and growth of a weaker structureless band centered at 657 nm attributed to the intermolecular PDI dimer.[22] A plot of the I_{549}/I_{657} fluorescence band intensity ratio vs the concentration of added NaCl is shown in the inset to Figure 3. The fluorescence quantum yields in buffer and in 100 mM NaCl are 0.009 ± 0.001 and 0.0005 ± 0.0002, respectively, similar to the values for the hairpin **H8** and its dimer.[22]

The circular dichroism spectra of **D8** in buffer and with added 100 mM NaCl are shown in Figure 4. The long-wavelength region of the CD spectrum in buffer displays a Cotton effect attributed to weak intramolecular exciton coupling between the two PDIs;[24] whereas the CD spectrum with added salt displays weak induced CD for the individual PDI chromophores similar to that for the dimer of hairpin **H8**.[22] The absence of strong intermolecular exciton coupling between stacked dumbbells is attributed to equal populations of chromophores having positive and negative angles between their electronic transition dipoles.[22] The short-wavelength region of the CD spectrum in buffer is similar to that for duplexes possessing short A-tracts, whereas the spectrum in the presence of 100 mM NaCl has a sharp intense band at 260 nm, similar to that for poly(dA)-poly(dT).[27]

The kinetics of **D8** assembly were studied by means of rapid mixing experiments conducted using a stopped-flow apparatus.

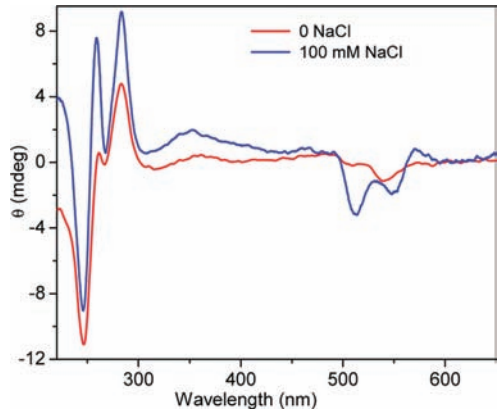

Figure 4. CD spectra of **D8** in 10 mM phosphate buffer (pH 7.2) in the absence and presence of 100 mM NaCl.

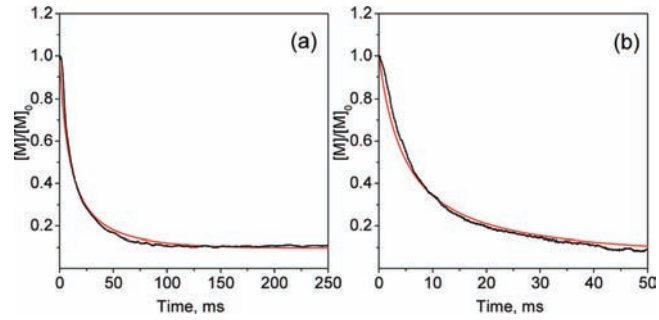

Figure 5. Plots of M/M_0 as a function of reaction time for mixing 3.0 μM **D8** with different concentrations of NaCl (a) 100 mM (b) 200 mM. Fitting curves obtained using an isodesmic polymerization model are shown in red.

Table 1. Association and Dissociation Rate Constants and Equilibrium Constants for Assembly of 3 μM **D8** in Buffer with Two NaCl Concentrations[a]

[NaCl] (mM)	k_a (M^{-1} s^{-1})	k_d (s^{-1})	K (M^{-1})
100	3.2×10^7	1.0	3.2×10^7
200	6.4×10^7	0.8	8.0×10^7

[a] Values of k_d and K obtained from fitting of Figure 5 using eq 1.

The assembly process was initiated by mixing a solution of **D8** (6 μM) in buffer with a solution of NaCl (200 or 400 mM) in buffer. The decrease in 540 nm absorbance was monitored following mixing. The absorbance was converted to the ratio M/M_0, where M_0 is the initial concentration of monomer, and M is its concentration at time t, as shown in Figure 5. The initial value of this ratio is normalized to 1.0, and the final ratio is determined from the UV A^{0-0}/A^{0-1} band intensity ratios in buffer and in the presence of 100 or 200 mM NaCl. Stopped-flow kinetic data for mixing of **D8** in buffer with NaCl can be fit to an isodesmic model[23] using eq 1 (see Supporting Information),

$$\frac{[M]}{[M]_0} = \left(\frac{\sqrt{1 + 4K[M]_0} - \dfrac{1}{\sqrt{1 + 4K[M]_0}}}{\dfrac{4}{e^{\sqrt{1 + 4K[M]_0}k_d t} - 1} + \dfrac{2}{\sqrt{1 + 4K[M]_0}} + 2} + 1 \right)^{-1} \quad (1)$$

where K is the equilibrium constant k_a/k_d. The fits of the stopped-flow data to eq 1 shown in Figure 5 provide the values of K, k_a, and k_d reported in Table 1. The difference between the experimental data and fit at short times may reflect either the

(26) Zhao, H. M.; Pfister, J.; Settels, V.; Renz, M.; Kaupp, M.; Dehm, V. C.; Wurthner, F.; Fink, R. F.; Engels, B. *J. Am. Chem. Soc.* **2009**, *131*, 15660–15668.
(27) Gudibande, S. R.; Jayasena, S. D.; Behe, M. J. *Biopolymers* **1988**, *27*, 1905–1915.

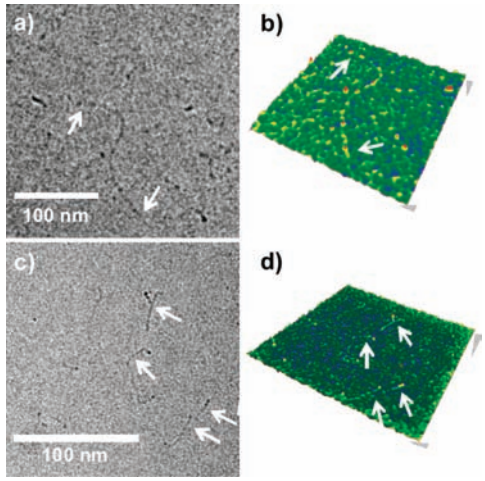

Figure 6. Cryo-TEM images of **D8** (3 μM) in 10 mM phosphate buffer/THF (9:1 v/v) mixture containing 100 mM NaCl. (b, d) show the 3D intensity profile of images (a, c), respectively.

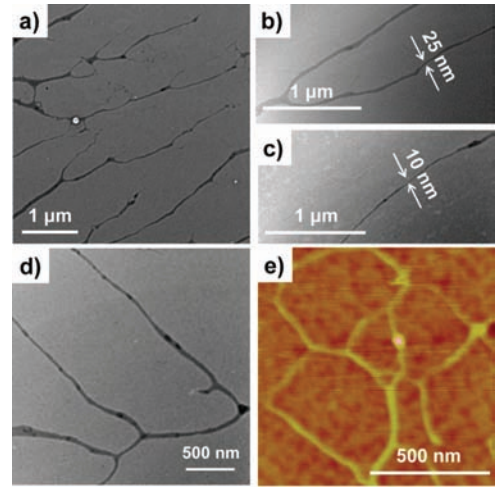

Figure 7. (a−d) TEM and (e) AFM images of the aggregates of **D8** (3 μM) obtained from solutions in 10 mM phosphate buffer containing 100 mM NaCl. The *z*-scale of the AFM image is 10 nm.

mixing time of the stopped-flow experiment or a different equilibrium constant for dimerization vs the subsequent chain growth steps.[23,28]

Dumbbell Assembly Structures. The structures of the **D8** assemblies have been investigated both by cryo-TEM and by conventional TEM and AFM. Structures observed by cryo-TEM for a solution of 3 μM **D8** in buffer containing 10% THF (by volume) with 100 mM NaCl are shown in Figure 6. The addition of THF improves the image quality but does not lead to significant disaggregation, as evidenced by the similar UV spectra obtained with and without added THF. Images were taken at −178 °C with 29K magnification (see Experimental Section). Samples were unstable at the higher electron flux required for higher magnification. Several structures having a width of ∼2.5 nm and a range of lengths from 30−100 nm as defined by darker termini can be identified in Figure 6a,c. Other structures which display a single darker terminus presumably are not entirely within the plane of focus.

TEM and AFM images obtained from solutions of 3 μM **D8** in buffer containing 100 mM NaCl are shown in Figures 7 and S4 (Supporting Information). Both the TEM and AFM images display branched structures having widths of 10−100 nm with linear regions >1 μm in length. The TEM images also display four-way junctions or fiber crossing. Section analysis of the AFM images (Figure S4e,f, Supporting Information) shows heights of ∼0.5 nm and widths of ∼50 nm.

Discussion

End-to-End Assembly in Dilute Solution. The UV and fluorescence spectra of **D8** in buffer are similar to those of hairpin **H8** in buffer and to those of other PDI monomers in organic solvents.[22,24] Similarly, the spectra of **D8** in the presence ≥100 mM NaCl are similar to those of **H8** and other PDI dimers and higher aggregates in organic solvents.[12,22] The high A^{0-0}/A^{0-1} band intensity for **D8** requires that most of its PDI chromophores exist as dimers or higher aggregates at high salt concentrations. Evidence for the formation of extended end-to-end assemblies in the presence of 100 mM NaCl is provided by the cryo-TEM images shown in Figure 6. These images show the presence of structures with diameters of ∼2.5 nm, corresponding to the width of a single strand of duplex DNA, and lengths of 30−100 nm, corresponding to the end-to-end assembly of ∼10−30 **D8** monomers. These structures display varying degrees of curvature; however, no circular structures were observed. The use of AFM and cryo-TEM to obtain images of single molecules of plasmid DNA has been reported.[29] However, we are unaware of prior reports of imaging of duplex assemblies as small as those shown in Figure 6.

The UV−vis and fluorescence spectra of **D8** in 100 mM NaCl are also consistent with the formation of long end-to-end assemblies. An average assembly size of 20 dumbbells would result in an internal/terminal PDI ratio of 38/2, consistent with the observation of an A^{0-0}/A^{0-1} band intensity ratio of 0.60 in buffer with 100 mM NaCl, slightly larger than the value of 0.55 for the dimer of **H8**,[22] which has no PDI end groups. The I_{549}/I_{657} fluorescence band intensity in the presence of 100 mM NaCl is ∼0.5 (Figure 3, inset). When corrected for the larger peak area and smaller fluorescence quantum yield for assembly vs monomer (0.0005 vs 0.009), this ratio also corresponds to an assembly size of ≥20 monomer units. The CD spectrum of the aggregate in buffer with 100 mM NaCl displays stronger, sharper bands in the 220−300 nm wavelength region dominated by the DNA A-tracts than does the spectrum in buffer (Figure 4). Particularly notable is the very strong, sharp 260-nm band which is a signature of very long A-tracts.[27,30] This suggests that the PDI chromophores mediate electronic interactions between the base pair domains of the individual dumbbells or that the end-to-end assembly is more conformationally rigid than the monomer.

The effect of added salt on the mole fraction of associated PDI chromophores (α_{ass}) can be calculated from the UV−vis absorption spectra (Figure 2a, inset), using values of the A^{0-0}/A^{0-1} band intensity ratio for the PDI monomer and assembly similar to those of hairpin **H8** and its dimer.[22,31] The calculated

(28) Henderson, J. R. *J. Chem. Phys.* **2009**, *130*, 045101.

(29) (a) Hansma, H. G.; Vesenka, J.; Siegerist, C.; Kelderman, G.; Morrett, H.; Sinsheimer, R. L.; Elings, V.; Bustamante, C.; Hansma, P. K. *Science* **1992**, *256*, 1180–1184. (b) Dubochet, J.; Adrian, M.; Dustin, I.; Furrer, P.; Stasiak, A. *Methods Enzymol.* **1992**, *211*, 507–518. (c) Neaves, K. J.; Huppert, J. L.; Henderson, R. M.; Edwardson, J. M. *Nucleic Acids Res.* **2009**, *37*, 6269–6275.

(30) Johnson, W. C. In *Landolt-Börnstein, Group VII*; Saenger, W., Ed.; Springer-Verlag: Berlin, 1990; Vol. I pp 1−24.

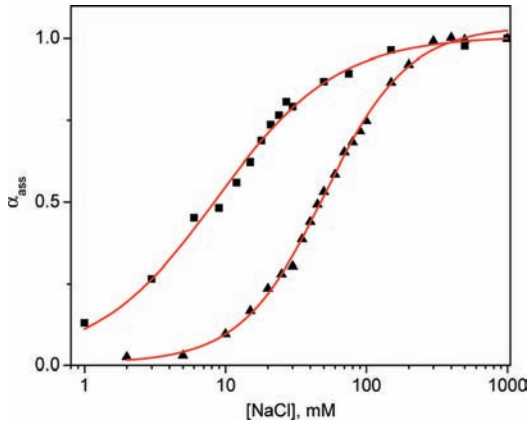

Figure 8. Salt dependence of the mole fraction of associated chromophores (α_{ass}) for **D8** (■) and **H8** (▲).

salt dependence of the mole fraction of aggregate (α_{ass}) is shown in Figure 8 along with our data for dimerization of the hairpin **H8**.[22] A NaCl concentration of ~10 mM is sufficient to effect approximately equal concentrations of monomer and aggregated PDI chromophores, corresponding to an average aggregate size of 2. This salt concentration is smaller than that needed to obtain a value of $\alpha_{ass} = 0.5$ for **H8** (~50 mM NaCl)[22] or for the conversion of a 14-mer hairpin having a tetranucleotide loop to the corresponding duplex (~100 mM NaCl).[32]

The effect of salt on the hairpin-to-duplex interconversion of the 14-mer hairpin was attributed to an increase in cation condensation about the central base-paired region of the duplex vs the disordered loop region of the hairpin.[32] Cation condensation could also play a role in the assembly of **D8**.[33] However, association of the large hydrophobic PDI chromophores presumably contributes significantly to the salt effect for aggregation of **D8** (Figure 8). The concentration and temperature dependence of the A^{0-0}/A^{0-1} band intensity ratio for 1 μM **D8** (Figures S1,2, Supporting Information) indicates that the monomer dumbbell is sparingly soluble under these conditions. Thus either an increase in **D8** concentration or a decrease in temperature will also shift the equilibrium between monomer and end-to-end assemblies (Figures S2,3, Supporting Information). Higher salt concentrations will increase the hydrophobic effect, a phenomenon known as electrostriction or, more commonly, as salting-out.[34]

Mechanism of Assembly. The assembly of **D8** conforms to the general characteristics of an isodesmic supramolecular polymerization (Figure 9), including the reversible nature of aggregation and the absence of either a critical concentration or critical temperature for self-assembly.[15,23,35] Reversibility and the absence of a critical concentration distinguishes the self-assembly of **D8** from the salt-induced conversion of cyanine dyes to their J-aggregates or assembly of DNA-bound porphyrins.[36,37] The values of K and k_a for **D8** are approximately twice as large for 200 vs 100 mM NaCl; whereas the values of k_d are similar (Table 1). Salt-jump kinetic measurements have previously been employed to study the hairpin-to-duplex transition of $d(A_6T_6)$ and related 12-mers.[38] Rate constants for this transition are also faster in 200 vs 100 mM NaCl (1.5×10^5 vs 0.5×10^5 $M^{-1}s^{-1}$). The observed salt dependence for **D8** assembly is consistent with both increased cation condensation and increased PDI hydrophobicity at higher salt concentrations.

The value of K for **D8** in buffer with 100 mM NaCl is substantially larger than the value reported for dimerization of hairpin **H8**,[22] indicative of stronger association for the difunctional dumbbell. By way of comparison, both k_a and k_d for **D8** assembly are significantly faster that the rate constants for hybridization and dehybridization of a 10-mer duplex in 1.0 M NaCl at 25 °C reported by Morrison and Stols ($k_a = 8.1 \times 10^6$ M^{-1} s^{-1} and $k_d = 2.0 \times 10^{-3}$ s^{-1}).[39] However, the value of K is larger for the 10-mer duplex ($K = 4 \times 10^9$ M^{-1}) than for **D8**.[39] A slower rate constant for hybridization ($k_a = 1.2 \times 10^6$ M^{-1}) has been reported for a 25-mer duplex at 20 °C in 0.5 M NaCl.[40] The smaller values of k_a for duplex formation plausibly reflect the greater solvent reorganization energy for base pairing vs PDI assembly.

TEM and AFM images obtained at room temperature following evaporation of solutions of 3 μM **D8** in buffer containing 100 mM NaCl shown in Figures 7 and S4 (Supporting Information) display branched structures with linear segments >1 μm in length and diameters between 10−100 nm. The branching points consist of globular features with diameters of 50−200 nm. The thinnest linear features have diameters of ~10 nm, similar to those reported for fibers of poly(rA)-poly(rU) and for the columnar phases of DNA duplexes.[9,10] These fibers consist of seven duplexes arranged in a close-packed hexagonal array surrounding a central duplex. STM images of DNA and RNA fiber bundles have revealed the presence of individual duplex strands;[3,41] however, the lower resolution of our TEM and AFM images is not sufficient to do so. A hexagonal packing mode can account for the formation of linear **D8** fibers having a diameter of ca. 10 nm (Figure 10). Assembly of several hexagonal bundles can account for the observation of branched structures having larger diameters. The curvature observed in the cryo-TEM images of single strand assemblies plausibly reflects the lack of packing constraints present in the hexagonal bundles.

Concluding Remarks

The PDI-linked dumbbell **D8** undergoes end-to-end assembly in dilute aqueous solution in the presence of NaCl (Figure 9). Cryo-TEM images obtained in the presence of 100 mM NaCl show the presence of assemblies consisting of 10−30 **D8** monomers (Figure 6). Assemblies of this size are consistent with

(31) The mol fraction of dimer at any concentration of NaCl can be determined from the equation $\alpha_{dim} = (\chi_0-\chi_c)/(\chi_0-\chi_\infty)$, where χ_0 is the ratio A^{0-0}/A^{0-1} (or I_{549} nm/I_{657} nm) in the absence of added salt, χ_c is the ratio in the presence of added salt, and χ_∞ is the ratio extrapolated to infinite salt concentration.

(32) Nakano, S.; Kirihata, T.; Sugimoto, N. *Chem. Commun.* **2008**, 700–702.
(33) Tan, Z. J.; Chen, S. J. *Biophys. J.* **2006**, *90*, 1175–1190.
(34) (a) Long, F. A.; McDevit, W. F. *Chem. Rev.* **1952**, *51*, 119–169. (b) Breslow, R. *Acc. Chem. Res.* **1991**, *24*, 159–164. (c) Zhu, H.; Lewis, F. D. *Bioconjugate Chem.* **2007**, *18*, 1213–1217.
(35) Fox, J. D.; Rowan, S. J. *Macromolecules* **2009**, *42*, 6823–6835.
(36) Chibisov, A. K.; Gorner, H.; Slavnova, T. D. *Chem. Phys. Lett.* **2004**, *390*, 240–245.
(37) (a) Slavnova, T. D.; Chibisov, A. K.; Gorner, H. *J. Phys. Chem. A* **2005**, *109*, 4758–4765. (b) Pasternack, R. F.; Gibbs, E. J.; Collings, P. J.; dePaula, J. C.; Turzo, L. C.; Terracina, A. *J. Am. Chem. Soc.* **1998**, *120*, 5873–5878.
(38) Zuo, E. T.; Tanious, F. A.; Wilson, W. D.; Zon, G.; Tan, G. S.; Wartell, R. M. *Biochemistry* **1990**, *29*, 4446–4456.
(39) Morrison, L. E.; Stols, L. M. *Biochemistry* **1993**, *32*, 3095–3104.
(40) Gao, Y.; Wolf, L. K.; Georgiadis, R. M. *Nucleic Acids Res.* **2006**, *34*, 3370–3377.
(41) (a) Lee, G.; Arscott, P. G.; Bloomfield, V. A.; Evans, D. F. *Science* **1989**, *244*, 475–477. (b) Lindsay, S. M.; Thundat, T.; Nagahara, L.; Knipping, U.; Rill, R. L. *Science* **1989**, *244*, 1063–1064.

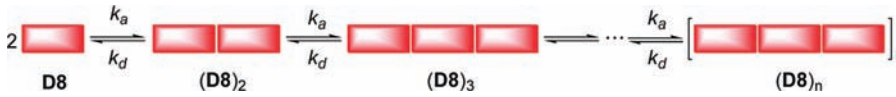

Figure 9. Isodesmic model for the salt-induced linear end-to-end assembly of **D8**.

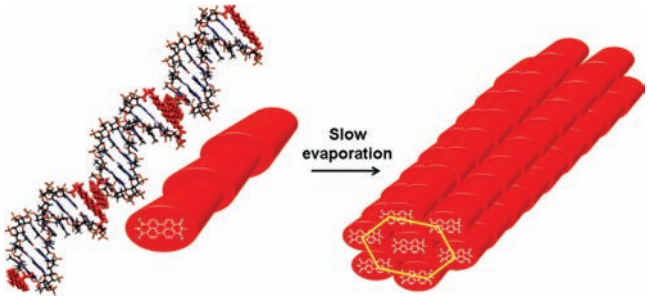

Figure 10. Schematic representation of the higher-order hexagonal-type aggregate formation of **D8** from initially formed short linear oligomers.

our analysis of the salt concentration dependence of the UV−vis (Figures 2 and 8) and fluorescence spectra of **D8** (Figure 3). The equilibrium between monomer and assembled **D8** is dependent upon temperature (Figure S3, Supporting Information) as well as the initial monomer (Figure S2, Supporting Information) and salt concentration. These observations provide the first example of the use of hydrophobic association for the assembly of small DNA duplex conjugates. In dried samples, **D8** forms branched assemblies with linear regions >1 μm in length and diameters as small as 10 nm, indicative of the formation of hexagonal bundles (Figure 10). Assembly of unmodified duplex DNA into small fibers or liquid crystals occurs only at much higher concentrations of duplex and salt.[10]

The assembly of **D8** occurs via the supramolecular polymerization of monomers containing PDI end groups separated by an 8-mer A-tract base paired duplex domain (Figure 1f). Supramolecular polymerization has been reported for the assembly of monomers possessing electronically noncoupled end groups via hydrogen bonding and other noncovalent interactions.[15] However, we are unaware of previous examples of one-dimensional supramolecular polymerization via pairwise stacking of hydrophobic PDI chromophores, which is difficult to achieve as PDI tends to form larger aggregates.[14] Negative charge repulsion limits the assembly of **D8** to a single strand under the conditions used for spectroscopic and cryo-TEM studies. Similarly, whereas there are previous examples of salt-induced aggregation, they occur via nucleation mechanisms.[37] The kinetics of **D8** assembly, as determined by stopped-flow mixing of **D8** with NaCl (Figure 5), are consistent with a salt-triggered isodesmic mechanism in which each reversible association step has the same rate constant (eq 1, Figure 9). Both the association and dissociation rate constants (Table 1) are faster than those for salt-induced hybridization of self-complementary DNA; however, the equilibrium constant for PDI association is smaller than that for DNA hybridization.[39] The rapid, reversible assembly of DNA/organic dye hybrids based on hydrophobic interactions leads to the formation of one-dimensional supramolecular polymers based on a single A-tract of DNA. Such systems are observed for the first time, providing entry into a new class of DNA-based assemblies. These one-dimensional polymers have an uninterrupted array of π-stacked aromatic chromophores composed of base pairs and PDI and thus may have interesting electronic properties.

Acknowledgment. This work was supported by grants from the National Science Foundation (NSF-CRC Grant No. CHE-0628130 to F.D.L.) and the Israel Science Foundation. The cryo-TEM studies were conducted at the Irving and Cherna Moskowitz Center for Nano and Bio-Nano Imaging (Weizmann Institute). AFM and TEM measurements were performed in the NIFTI facility of NUANCE Center and the Biological Imaging Facility (BIF) at Northwestern University, respectively.

Supporting Information Available: Experimental Section, Figures S1−S4, and the derivation of eq 1. This material is available free of charge via the Internet at http://pubs.acs.org.

JA1076525